

## THE SPHERICAL PROBE ELECTRIC FIELD AND WAVE EXPERIMENT

G. Gustafsson<sup>5</sup>, T. Aggson<sup>8</sup>, R. Boström<sup>1</sup>, L.P. Block<sup>4</sup>, C. Cattell<sup>2</sup>, P. Décréau<sup>12</sup>, A. Egeland<sup>7</sup>, C-G Fälthammar<sup>4</sup>, R. Grard<sup>8</sup>, D. Gurnett<sup>11</sup>, C. Harvey<sup>14</sup>, B. Holback<sup>1</sup>, G. Holmgren<sup>1</sup>, P. Kellogg<sup>15</sup>, P. Kintner<sup>13</sup>, S. Klimov<sup>16</sup>, J-P Lebreton<sup>3</sup>, P-A Lindqvist<sup>4</sup>, R. Manning<sup>14</sup>, G. Marklund<sup>4</sup>, N. Maynard<sup>5</sup>, F. Mozer<sup>2</sup>, K. Mursula<sup>6</sup>, A. Pedersen<sup>3</sup>, R. Pfaff<sup>6</sup>, I. Roth<sup>2</sup>, A. Roux<sup>10</sup>, R. Schmidt<sup>3</sup>, H. Singer<sup>5</sup>, M. Smiddy<sup>5</sup>, K. Stasiewicz<sup>1</sup>, P. Tanskanen<sup>6</sup>, M. Temerin<sup>2</sup>, E. Thrane<sup>7</sup>, J. Wygant<sup>2</sup>, L.J.C. Woolliscroft<sup>9</sup>

1: Swedish Inst. of Space Physics, Uppsala, Sweden

2: Univ. of California, Berkeley, CA 94720, USA

3: SSD/ESTEC, Noordwijk, The Netherlands

4: The Royal Inst. of Techn., Stockholm, Sweden

5: Air Force Geophysics Lab., MA 01732, USA

6: Univ. of Oulu, Oulu, Finland

7: Univ. of Oslo, Oslo, Norway

8: NASA, GSFC, Greenbelt, MD 20771, USA

9: Univ. of Sheffield, U.K.

10: CRPE/CNET, Issy-les-Moulineaux, France

11: Univ. of Iowa, Iowa 52242, USA

12: LPCE/CNRS, Orléans, France

13: Cornell Univ., Ithaca, NY 14853, USA

14: Observatoire de Paris-Meudon, France

15: Univ. of Minnesota, Minneapolis, USA

16: Space Research Inst., Moscow, USSR

### Abstract

The electric field and wave experiment (EFW) on Cluster is designed to measure the electric field and density fluctuations with sampling rates, on some occasions, up to 40000 samples/s in two channels. Langmuir sweeps can also be made to determine the electron density and temperature. Among the more interesting objectives of the experiment is to study nonlinear processes that result in acceleration of plasma. Large scale phenomena where all four spacecraft are needed will also be studied.

Keywords: Electric field, Electron density, Waves, Boundaries, Cluster mission.

### Scientific Background

#### Introduction

The CLUSTER spacecraft will pass through numerous plasma regimes separated by a variety of boundaries and discontinuities. From the view point of an electric field and plasma fluctuation experiment, this means that a large variety of wave-wave, wave particle and nonlinear plasma interactions as well as time and space variations of macroscopic and quasi-static electric fields will be found along the trajectory of the space craft. These phenomena will occur over widely differing temporal, spatial, and amplitude ranges. To provide an adequate understanding of the phenomena, an electric field and plasma fluctuation experiment must be able to measure, in two dimensions, over frequencies ranging from DC to 10 kHz with a time resolution of 100 microseconds. This will cover waves up to lower hybrid modes, and the time resolution will resolve time domain structures. Amplitudes of a few  $\mu$  V/m to 700 mV/m has to be covered and plasma density fluctuations from about 1 to 50 % relative variation. It should be able to measure phase velocities of electrostatic structures

over time scales of milliseconds by interferometric timing between opposing boom pairs. In order to measure the polarization of electrostatic waves and resolve the k vectors of waves propagating perpendicular and parallel to the magnetic field with frequencies faster than the spin rate of the spacecraft, it must have two pairs of electric field sensors which can be sampled to produce an instantaneous two dimensional electric field vector. The operation mode with all four probes measuring density fluctuations, will allow two dimensional plasma wave interferometer measurements to determine wavelength, phase velocities and time of flight of plasma phenomena. Finally, it must have an internal burst memory in order to record high time resolution data at rates higher than the telemetry stream. This burst memory should be large enough to sample over the spatial distances associated with the bow shock, auroral structures, the plasma sheet boundary, and the magnetopause.

The experiment has four spherical sensors located at the end of 50 m long booms in the spin plane of the satellite. It covers four basic frequency ranges with two analog-to-digital converters that can sample up to 40 k samples/s and it has an internal memory of one megabyte.

#### Electric Fields at Small Scales

Some of the most interesting magnetospheric physics is associated with nonlinear processes that result in the acceleration of plasma. S3-3, Viking and ISEE electric field measurements have shown that particle acceleration is associated with large amplitude, short duration electric field signatures see Figures 1 and 2. Small spatial and temporal scale structures are important because they provide the necessary dissipation in the various magnetospheric boundary regions. They are equally important, from the view of basic plasma physics. They represent the nonlinear state of the plasma under various conditions and as such are at

the forefront of basic plasma physics.

Since such structures are inherently nonlinear, it is desirable to study them in the time domain. The use of time domain information nicely complements the spectral information that is important in the study of linearly propagating waves. The investigation of nonlinear structures in the time domain provides the best opportunity to make new discoveries by exploiting the capabilities allowed by recent advances in technology.

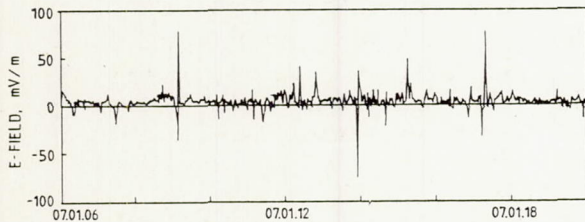


Figure 1 Measurements on ISEE-1 at 32 samples/sec of spiky electric fields of about 100 mV/m and a duration of 0.05 seconds of a bow shock crossing. This is a single axis measurement so that the direction relative to the magnetic field of the spikes is not known. Similarly no information of the phase velocity is available from this measurement. On Cluster the phase velocity could be determined if the potentials from each of the four probes were available at sampling rates of 10000 times/sec.

ISEE observations in the bow shock reveal intense electric field spikes with amplitudes of 100 mV/m and durations of .05 second (Figure 1). The spikes are often bipolar. Almost none of the properties of these waves can be determined by the ISEE experiment but could be determined by the Cluster quasi-static experiment. The phase velocity, scale size, polarization relative to the ambient magnetic field, three-dimensional structure, coherence length, relation to comparable temporal scale density and magnetic field fluctuations can be determined with the Cluster electric field instrument in four satellites. These quantities are needed to evaluate the role of the spikes in providing anomalous resistivity, thermalizing ion and electron distributions, and in the production of high energy electron beams commonly seen at the bow shock.

High time resolution data must be obtained using the internal burst memory in various different sampling schemes based on the region of space being sampled. Whenever higher-time resolution data have become available, new phenomena have been discovered, e.g. recent rocket observations of Langmuir solitons (Ref. 1). We anticipate the discovery of many interesting important new structures in the high-frequency time domain data to be obtained by the Cluster satellites.

#### Electric Fields at Intermediate Scales

Many of the central scientific goals of the Cluster mission relate to electric fields at intermediate scales (100's of km

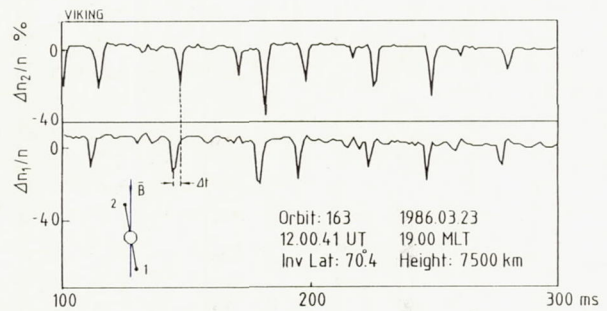


Figure 2 These measurements from Viking show high time resolution density fluctuation data in two channels. The instrument could also measure one electric field vector and one density fluctuation parameter simultaneously. From these data rather detailed characteristics of weak double layers could be obtained such as propagation velocity and direction, scale length, net electric field etc. (Ref. 14). On Cluster similar phenomena could be studied in other regions of space and scale lengths in two direction with a time resolution of a millisecond or better.

to a few  $R_E$ ). These include MHD turbulence in the solar wind, magnetosheath and cusp, instabilities driven by velocity shears, waves associated with quasi-parallel shocks, transfer events, impulsive penetration of plasma into the magnetosphere, and slow mode shocks in the near tail in association with reconnection. Electric field data will provide information which is vital for determining wave modes, wave vectors, phase velocities and energy flow. The spatial and temporal variation in the auroral zone electric field is another interesting topic addressed by measurements on these spatial scales.

The average behavior of the auroral zone electric field and related electro-dynamical parameters for various geophysical conditions is relatively well documented. This is, however, not the case for the instantaneous auroral electro-dynamics on which very few studies have been conducted (Refs. 2, 3). A new technique to obtain global realistic and self-consistent distributions of auroral electro-dynamical parameters has been recently developed (Ref. 3). Simultaneous observations on the different spacecraft involved are used both for calibration of the model input data (field-aligned currents and conductivities) and for tests of the results (equipotential pattern). For these kinds of studies the Cluster mission with simultaneous four-point measurements will be ideally suited.

The electric field is an important parameter in the measurement of MHD turbulence. MHD turbulence is expected in all the important regions to be investigated by Cluster. The electric field, together with the magnetic field, determines the Poynting flux and the propagation direction of the waves and plasma flows in these regions. The scale size and the magnitude of the electric fields involved have a wide range of values in these various regions. In the solar wind, scale sizes are several hundred kilometers to many thousands of kilometers and electric field magnitudes are of the order of 1 mV/m. On auroral field lines,

the electric field is typically much larger. Magnitudes of over 100 mV/m are common on scale sizes from less than a kilometer to tens of kilometers (Refs. 4, 5, 6). The quasi-parallel shock structure provides a strong challenge to space physicists attempting to understand the role of different wave modes and scale sizes in the deceleration and thermalization of upstream plasma. The four Cluster spacecraft can determine the phase velocity and Poynting flux waves and "shocklets" upstream and downstream of the shock. In the absence of such measurements it would be difficult to distinguish between waves standing in the shock frame, those waves created in the upstream region and convected and amplified across the shock transition region, and those waves created in the transition region.

#### Electric Fields at Large Scales

At the longest scale lengths of interest for the Cluster study are the electric fields associated with processes such as steady-state reconnection at the magnetopause, convection in the "quiet" magnetotail, and the formation of a near-earth neutral line.

Steady-state convection in the magnetotail has been examined using analytic and numerical methods as well as simulations (Refs. 7, 8). Their models will be testable for the first time using the Cluster electric field data. ISEE-1 electric field data have suggested that the electric fields associated with the hypothesized near-earth neutral line are confined to  $\approx 10 - 15R_E$  in the dawn-dusk direction (Refs. 9, 10). Comparisons of observed electric fields in the tail (20-40 mV/m during candidate neutral line events) with cross-polar-cap potentials imply that the field is primarily inductive (Refs. 10, 11). The Cluster satellite electric and magnetic field data will allow direct determination of associated electric fields, the relative importance of inductive and potential fields, as well as the relationship of the neutral line propagation speed to the electric field and where reconnection is initiated in the plasma sheet. The four satellites will also be able to determine the extent of substorm electric fields which may not be directly related to the neutral line (Ref. 12), in particular how these fields are related to substorm injection. Preliminary results on the propagation of these electric fields by comparing the ISEE-1 and GEOS data have been provided (Ref. 11). Comparisons of the  $E \times B$  velocity to plasma sheet boundary motions (Ref. 13) have shown that the two agree during plasma sheet contraction, but not during expansion. Cluster electric field data can provide additional, more detailed information for understanding plasma sheet-motion, in particular, variations in the dawn-dusk and earthward-tailward directions.

#### Instrument Description

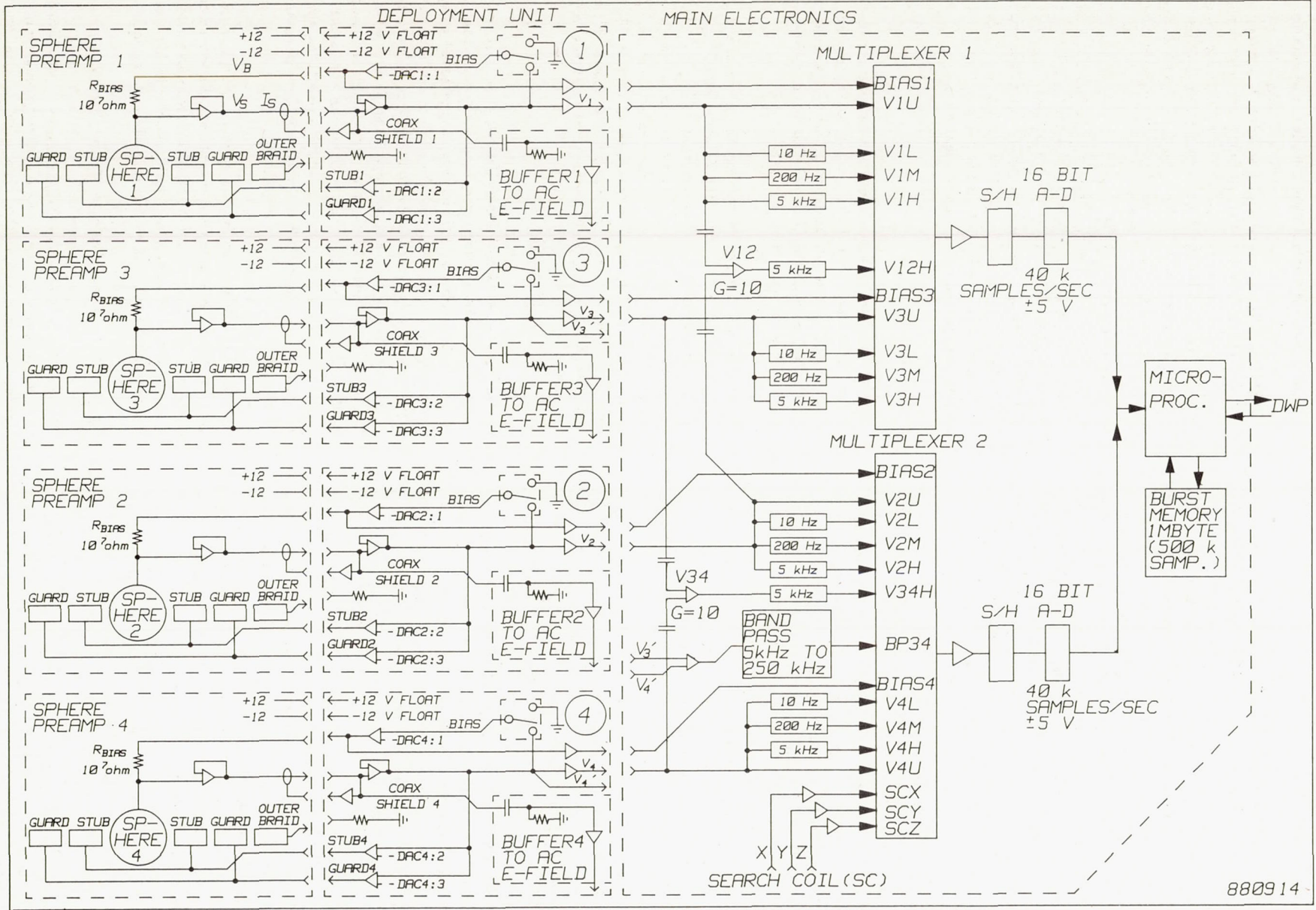
##### General

To meet the scientific objectives the electric field instrument will be capable of measuring, in various modes;

- Instantaneous spin plane components of the electric field vector, over a dynamic range of 0.1 to 700 mV/m, and with variable time resolution down to 0.1 millisecond.
- The low energy plasma density, over a dynamic range at least 1 to 100  $\text{cm}^{-3}$ ;
- Electric fields and density fluctuations in double layers of small amplitude, over dynamic ranges of 0.1 to 50 mV/m for the fields and 1 to 50 percent for the relative density fluctuations, and with a time resolution of 0.1 millisecond on some occasions;
- Electric fields and density fluctuations in electrostatic shocks or double layers of large amplitude, over dynamic ranges of 0.1 to 700 mV/m for the fields and 1 to 50 percent for the relative density fluctuations, and with a time resolution of 0.1 millisecond on some occasions;
- Waves, ranging from electrostatic ion cyclotron emissions having amplitudes as large as 60 mV/m at frequencies as low as 50 millihertz, to lower hybrid emissions at several hundred Hertz and with amplitudes as small as a few  $\mu\text{V}/\text{m}$ ;
- Time delays between signals from up to four different antenna elements on the same spacecraft, with a time resolution of 25 microseconds on some occasions.
- The spacecraft potential.

The detector of the instrument consists of four orthogonal spherical sensors deployed from 50 meter cables in the spin plane of the spacecraft, four deployment units, and a separate main electronics unit as shown in the block diagram in Figure 3. The instrument has several important features. The potential drop between two opposing spherical sensors can be measured to provide an electric field measurement. The instrument can also be operated as a Langmuir Probe and biased to provide the Langmuir current-voltage curve and, thus, the electron temperature and density. The potentials of the spherical sensor and nearby conductors are controlled by the microprocessor in order to minimize errors associated with photoelectron fluxes to and from the spheres. The output signals from the spherical sensor preamplifiers are provided to the wave instruments for analysis of high frequency wave phenomena. The instrument has a 1-megabyte burst memory and two fast A/D conversion circuits for recording electric field wave forms for time resolutions up to 10 kHz. Data gathered in the burst memory will be played back through the telemetry stream allocated to the electric field experiment by preempting a portion of the real time data gathered by the instrument. On board calculations of least square fits to the electric field data over one spacecraft spin period (4 seconds) will provide a baseline of high quality two dimensional electric field components that are always present in the telemetry stream. Incoming data is continuously monitored using algorithms in software to determine if conditions are appropriate for triggering a burst collection playback.

Figure 3 Block diagram of EFW.



### Analog Electronics

Each sphere houses a preamplifier which measures the potential difference between the sphere surface and the spacecraft analog ground. Since the plasma has high source impedance ( $10^7 - 10^{10}$  ohms) and a capacitance of 5 picofarads due to the 8 cm diameter sphere, the preamplifier must have a low leakage current ( $< 10$  picoamperes) and low input capacitance ( $< 1$  picofarad) to avoid the attenuation of input signals. Since the potential of a biased sphere can differ from that of the spacecraft by 5-50 volts in the absence of an electric field, and fields as large as 500 mV/m have been observed, the dynamic range of the preamplifier and associated sensor electronics is  $\pm 70$  volts from DC to 300 Hz. The small signal response exists to 600 kHz for use by the AC electric field instrument.

The 50-meter boom cable between the deployment unit and the sphere sensors contains eight wires and one coaxial cable. These wires carry the power to the preamplifier in the sphere, the biasing voltages on the stub and guard surfaces, and the biasing voltage to the bias resistor. The wires and coaxial cable are surrounded by a kevlar braid which provides mechanical support against the centrifugal stresses on the cable. The outer surface of the cable is a conductor which is tied via a  $10^6$  ohm resistor to the spacecraft chassis. This resistance constitutes a negligible load for transmitters and receivers associated with the active sounder experiment or the inter-spacecraft link which may use the outer conductors on the 50 meter cables as antennae.

In order to limit and control the flux of photo-electrons from the booms to the spherical sensors and minimize error sources in the potentials of stub and guard surfaces are forced to follow the potential of the sphere with an adjustable DC offset. The DC offset is determined by 8 bit microprocessor-controlled digital-to-analog converters located in the digital section of the main electronics box. The stub voltage follows the sphere voltage with an offset which can range between -1.44 and +1.44 volts in 256 steps. The guard voltage follows the sphere potential with an offset between -35.6 and +35.6 volts in 256 steps.

The sphere potential is determined by the balance of plasma thermal currents, photoemission current, and a bias current to the sphere whose magnitude is controlled by on-board electronics to minimize the sheath impedance. This is accomplished by controlling the potential drop across a bias resistor,  $R$ , of Figure 3 with bias control circuitry. One end of the bias resistor is tied to the sphere surface. The other end of the resistor is driven by the bias control circuitry which operates in one of the two modes as determined by the state of a bias relay. If the instrument is measuring electric fields, the relay is set so that the bias control circuit follows the output of the sphere with a DC offset determined by the DAC. The potential drop across the resistor is the DAC determined value and the injected current is this value divided by the value of the resistance. This current can vary from -3.6 to +3.6 microamperes in 256 steps. These values are large enough to balance the

maximum possible photoelectron flux from the spheres.

The spherical sensors can also be operated as current collecting Langmuir probes to provide information on the plasma density and electron temperature. In this mode, relays in each of the four deployment units are flipped so that the microprocessor controlled bias circuits are referenced to the satellite rather than the output of the sphere preamplifier.

The output of each sphere preamplifier is filtered by anti-aliasing filters with frequencies at 10 Hz, 200 Hz, 5 kHz and 10 kHz. A simple frequency counter is included for the range 5-250 kHz. The low frequency filter data will be utilized for direct transmission of data. The 200 Hz signal will be stored on the on-board tape recorder. The highest frequency data will be recorded in the internal burst memory and played out at slower telemetry rates.

### Digital Electronics

The digital electronics contain two very fast analog-to-digital system, a set of digital-to-analog converters for biasing, a single 8-bit radiation-hard microprocessor, and a large burst memory. Extensive software functions increase the instrument's capabilities and data coverage.

The strategy for measuring the sphere voltages over a range of plus or minus 700 mV/meter to an accuracy of 1 microvolt/meter can be achieved in a number of ways. With a 16-bit converter, the single ended measurements of sphere voltage (V1 through V4) will be measurable from 350 mV/m to  $10 \mu$  V/m. Differential measurements V1-V2 and V3-V4 will have a gain factor of ten and thus be measurable to about  $1 \mu$  V/m but will only have a range to 10 mV/m.

### Boom Deployment Mechanism

Each DC Electric Fields Deployment Unit is a small, self-contained package containing a motor driven mechanism that deploys a multiconductor cable and tip mounted spherical sensor in the spin plane of the Cluster satellites. On orbit, each opposing pair of cables will be symmetrically deployed to a tip-to-tip distance of approximately 100 meters. The assembly consists of two major components: a deployment mechanism, and the cable with sensor. The mechanism design has evolved from a series of successful satellite experiments including S3-2 and S3-3, ISEE, Viking, and CRRES.

The deployment unit contains a rotating assembly, a brush DC gearmotor, an over-tension and end-of-cable indicator, an analog cable length indicator, a pyrotechnic-released spherical sensor housing, and a cable oscillation Coulomb damper through which the cable exits the mechanism.

### Distribution of responsibilities among institutes:

The laboratories in Berkeley, Noordwijk, Oslo, Oulu, Stockholm and Uppsala are responsible for the design, production, test and integration of hardware with support from Hanscom/AFGL. The main responsibility for software and data handling is with Berkeley, Greenbelt/GSFC, Oslo,

Stockholm and Uppsala. The institute in Moscow contributes to the coordination with the IKI-spacecraft. The institutes in Ithaca and Minneapolis are mainly contributing to theoretical support and co-investigators at other institutes not mentioned above contribute to the coordination with the wave consortium which EFW is a part of.

### Instrument Summary

The main characteristics of the instrument are the capability of high sampling rate, two-dimensional electric field measurements and two dimensional plasma interferometer measurements with four Langmuir probes.

### Measured quantities

Three main parameters will be measured.

- i) The quasi static Electric Field.
- ii) The Wave Electric Fields
- iii) The plasma Density and the relative Density Fluctuations

Measured quantity	Frequency range	Dynamic range
DC Electric Field (2 components)	0 - 10 Hz	700 mV/m - 0.1 mV/m
	0 - 200 Hz	700 mV/m - 0.1 mV/m
	0 - 5000 Hz	700 mV/m - 0.1 mV/m
	0 - 10000 Hz	700 mV/m - 0.1 mV/m
AC Electric Field (2 components)	10 - 5000 Hz	10 mV/m - $\approx 1 \mu\text{V/m}$ See note.
Plasma density fluctuations	0 - 10 Hz	1 - 100 $\text{cm}^{-3}$
	0 - 200 Hz	1 - 100 $\text{cm}^{-3}$
	0 - 5000 Hz	1 - 100 $\text{cm}^{-3}$
Density and Temperature (Langmuir sweeps)		1 - 100 $\text{cm}^{-3}$ eV range

Note: For gain = 10. Final gain not yet determined.

### Data rates

Nominal telemetry rate	1440 bits/sec
Tape Loading Mode Data Rate	$\leq 24$ kbits/sec
Burst Memory Loading Mode Data Rate	$\leq 1280$ kbits/sec

### Physical Data

Item	Mass (kg)	Power (W)
Main Electronics Box	1.96	3.1
Wire Booms 4 units	15.55	

### References

1. Boehm, M.H., C.W. Carlson, J. McFadden, and F.S. Mozer, *Geophys. Res. Lett.*, 11, 511, 1984.
2. Heelis, R.A., J.C. Foster, O. de la Beaujardiere, and J. Holt, *J. Geophys. Res.*, 88, 10, 111, 1983.
3. Marklund, G.T., R.A. Heelis, and J.D. Winningham, *Can. J. Phys.*, 64, 1417, 1986.
4. Block, L.P., C.-G. Fälthammar, P.-A. Lindqvist, G. Marklund, F.S. Mozer, and A. Pedersen, *Geophys. Res. Lett.*, 14, 435, 1987.
5. Fälthammar, C.-G., L.P. Block, P.-A. Lindqvist, G. Marklund, A. Pedersen, and F.S. Mozer, *Annales Geophysicae* 5 (4), 1987.
6. Marklund, G.T., L.G. Blomberg, T.A. Potemra, J.S. Murphree, F.J. Rich, and K. Stasiewicz, *Geophys. Res. Lett.*, 14, 329, 1987a.
7. Erickson, G.M., and R.A. Wolf, *Geophys. Res. Lett.*, 7, 900, 1980.
8. Schindler, R., and J. Birn, *J. Geophys. Res.*, 87, 2263, 1982.
9. Dhont, J., C.A. Cattell, and F.S. Mozer, *EOS*, 67, 1173, 1986.
10. Cattell, C.A., F.S. Mozer, E.W. Hones, Jr., R.R. Anderson, and R.D. Sharp, *J. Geophys. Res.*, 91, 5663, 1986.
11. Pedersen, A., C.A. Cattell, C.-G. Fälthammar, V. Formisano, P.-A. Lindqvist, F.S. Mozer, and R.B. Torbert, *Space Sci. Rev.*, 37, 269, 1984.
12. Cattell, C.A., and F.S. Mozer, in AGU Mon. # 30, 208, 1984.
13. Pedersen, A., C.A. Cattell, C.-G. Fälthammar, K. Knott, P.-A. Lindqvist, R.H. Manka, and F.S. Mozer, *J. Geophys. Res.*, 90, 1231, 1985.
14. Boström, R., G. Gustafsson, B. Holback, G. Holmgren, H. Koskinen, P. Kintner, *Phys. Rev. Lett.*, 61, 1988.